Backbone Conformational Preferences and Pseudorotational Ring Puckering of 1-Aminocyclopentane-1-carboxylic Acid

Carlos Alemán,*,† David Zanuy,*,† Jordi Casanovas,‡ Carlos Cativiela,§ and Ruth Nussinov∥,⊥

Departament d'Enginyeria Química, E. T. S. d'Enginyeria Industrial de Barcelona, Universitat Politècnica de Catalunya, Diagonal 647, Barcelona E-08028, Spain, Departament de Química, Escola Politècnica Superior, Universitat de Lleida, c/Jaume II N° 69, Lleida E-25001, Spain, Departamento de Química Orgánica, Instituto de Ciencia de Materiales de Aragón, Universidad de Zaragoza-CSIC, 50009 Zaragoza, Spain, Basic Research Program, SAIC-Frederick, Inc., Center for Cancer Research Nanobiology Program, NCI, Frederick, Maryland 21702, and Department of Human Genetics Sackler, Medical School, Tel Aviv University, Tel Aviv 69978, Israel

Received: May 8, 2006; In Final Form: August 18, 2006

We have used quantum mechanical calculations at the B3LYP/6-311G(d,p) level to determine the conformational preferences of the *N*-acetyl-*N*′-methylamide derivative of 1-aminocyclopentane-1-carboxylic acid in the gas phase, chloroform solution, and water solution. The backbone conformation of this dipeptide has been described through the dihedral angles φ and ψ, while the pseudorotational phase angle was used to define the conformation of the cyclopentane ring. Results indicate that the backbone flexibility of this amino acid is restricted by the cyclic nature of the side chain, the relative stability of the different conformations depending on the polarity of the environment. The potential energy of the pseudorotation was also studied as a function of the backbone conformation. Interestingly, the conformation of the cyclic side chain depends on the backbone arrangement. Furthermore, the number of pseudorotational states accessible at room temperature is high in all the investigated environments, especially in aqueous solution. Finally, a set of force-field parameters for classical molecular mechanics calculations was developed for the investigated amino acid. Molecular dynamics simulations in both chloroform and aqueous solutions were performed to demonstrate the reliability of such parameters.

Introduction

In recent years modern methods based on quantum mechanics have been extensively applied to provide an accurate description of the conformational properties of L-proline (Pro).[1] Proline is unique among the natural amino acids in that its nitrogen atom is fixed within a pyrrolidine ring that reduces the conformational flexibility of this amino acid with respect to most others. Furthermore, these conformational studies have been extended to 4-substituted proline derivatives such as 4(*R*)- and 4(*S*)-hydroxyproline and 4(*R*)- and 4(*S*)-fluoroproline.[2] Results have provided a useful picture about their intrinsic molecular properties in the absence of intermolecular interactions and have been examined in terms of not only amide cis−trans isomerism but also pyrrolidine ring puckering. Thus, the five-membered pyrrolidine moiety of Pro and its derivatives can adopt different down- and up-puckered conformations, which have been used to explain the interactions that govern the structure and dynamics of polypeptide chains containing such amino acids (for instance, collagen, the most abundant protein in vertebrates).[1,2]

Within a broad project devoted to re-engineering protein modules via targeted replacements with constrained amino acids for the generation of nanodevices,[3] we are interested in an amino acid that also contains a five-membered ring (Figure 1). This is the quaternary cyclic α-amino acid 1-aminocyclopentane-1-carboxylic acid (Ac_5c). Synthetic 1-aminocycloalkane-1-carboxylic acids (Ac_nc, where *n* indicates the size of the ring) are the result of $C^\alpha \leftrightarrow C^\alpha$ cyclization whereby dialkylated glycine residues with cyclic side chains are formed. The conformational properties of the simplest member of this series, 1-aminocyclopropane-1-carboxylic acid (Ac_3c), have been well-characterized using both experimental[4] and theoretical[5] methodologies. Studies of peptides containing the cyclopentane homologue, Ac_5c, indicate that this amino acid presents a restricted conformational space with a high propensity to adopt a set of φ,ψ backbone torsion angles typical of the 3_{10}-/α-helical region,[4a,b,6] while little attention has been paid to the conformational properties of the cyclic side chain.

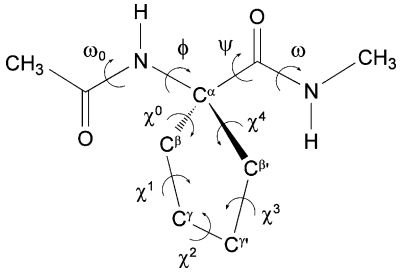

Figure 1. Structure of Ac−Ac_5c−NHMe indicating the backbone and endocyclic dihedral angles.

A distinctive structural feature of Ac_5c is that the backbone dihedral angles φ,ψ are not as geometrically restricted by the

* Authors to whom correspondence should be addressed. E-mail: carlos.aleman@upc.edu; david.zanuy@upc.edu.
† Universitat Politècnica de Catalunya.
‡ Universitat de Lleida.
§ Universidad de Zaragoza-CSIC.
∥ NCI.
⊥ Tel Aviv University.

10.1021/jp062804s CCC: $33.50
Published on Web 09/23/2006

five-membered cycle as in Pro, even though the steric interactions produced by this bulky side group are expected to constrain its conformational flexibility. Conversely, the puckering of the cyclopentane system may be influenced by the backbone conformation. In this work, we present a detailed and systematic study of the conformational preferences of the *N*-acetyl-*N*′-methylamide derivative of Ac_5c ($Ac-Ac_5c-NHMe$) using density functional theory (DFT) calculations. To figure out how the conformational propensities of Ac_5c are influenced by the interactions between the backbone atoms and the cyclopentane ring, the latter has been specifically characterized for every backbone minimum energy conformation by using the pseudorotation concept.[7] Furthermore, the influence of the polarity of the environment on the conformational preferences has been examined using a self-consistent reaction-field (SCRF) method. Finally, a set of force-field parameters has been developed for Ac_5c to allow molecular dynamics simulations (MD). The suitability of such parameters has been checked by comparing the conformational preferences predicted for $Ac-Ac_5c-NHMe$ by DFT calculations and MD simulations.

Methods

All calculations were carried out using the Gaussian 03 computer program.[8] DFT calculations were performed using the following combination: Becke's three-parameter hybrid functional (B3)[9] with the Lee, Yang, and Parr (LYP)[10] expression for the nonlocal correlation (B3LYP). Thus, all the calculations presented in this work were performed using the B3LYP method combined with the 6-311G(d,p) basis set.[11]

Torsion angles for the backbone and cyclopentane ring of $Ac-Ac_5c-NHMe$ are defined in Figure 1. Because each flexible backbone dihedral angle is expected to have three minima, i.e., gauche$^+$ (60°), trans (180°), and gauche$^-$ (−60°), the number of minima that may be anticipated for the potential energy hypersurface $E = E(\varphi,\psi)$ of $Ac-Ac_5c-NHMe$ is $3^2 = 9$. Furthermore, due to the cyclic nature of the side chain, two envelope (*E*) arrangements of the cyclopentane side chain are expected for each backbone minimum energy conformation. Accordingly, such $9 \times 2 = 18$ structures were considered as starting points for complete geometry optimizations at the B3LYP/6-311G(d,p) level. This systematic conformational analysis strategy has allowed us satisfactory exploration of the potential energy hypersurfaces not only of small dipeptides[5a,c,12] but also of flexible organic molecules.[13] Frequency analyses were carried out to verify the nature of the minimum state of all the stationary points obtained and to calculate the zero-point vibrational energies (ZPVE) and both thermal and entropic corrections. These statistical terms were used to compute the conformational Gibbs free energies in the gas phase (ΔG^{gp}) at the B3LYP/6-311G(d,p) level.

The pseudorotation[7] of the cyclopentane ring has been described following the formalism of Altona and Sundaralingam,[14] which is based on two mathematical parameters and the phase angle of pseudorotation (*P*). Accordingly, the conformations of the five endocyclic ring torsion angles (χ^i with $i = 0-4$; Figure 1) have been related to τ_m and *P* through the simple trigonometric expression:

$$\chi^i = \tau_m \cos(P + 0.8\pi(i - 2)) \qquad (1)$$

where *P* may range from 0 to 2π and τ_m is the amplitude of the puckering (typically $\tau_m \approx 40°$).[14,15] However in this work, *P* is referred to in units of degrees. To determine the potential energy of the pseudorotation for each backbone conformation, the endocyclic torsion angles χ^1 and χ^2 were constrained. For this purpose, values for χ^1 and χ^2 were calculated for each point along the pseudorotation pathway using eq 1 and $\tau_m = 40°$. Other alternative formulations to describe the ring puckering have been proposed, that provided by Cremer and Pople being specially relevant.[16a] In this method the geometry of the puckering relative to a mean plane is defined by amplitude and phase coordinates that are generalizations of those introduced for cyclopentane by Kilpratick et al.[16b] However, the method of Altona and Sundaralingam[14] is the simplest to identify the conformers of five-membered rings in terms of endocyclic dihedral angles. The profiles were obtained through full geometry optimizations of the pseudorotameters at the B3LYP/6-311G(d,p) level while maintaining the desired χ^1 and χ^2 angles. No restraints were placed in the backbone dihedral angles.

The pseudorotational parameter *P* of the $Ac-Ac_5c-NHMe$ minimum energy conformations was obtained through the following expression:

$$\tan P = \frac{\chi^1 + \chi^4 - \chi^0 - \chi^3}{3.077683\chi^2} \qquad (2)$$

To obtain estimation of the solvation effects on the relative stability of the different minima, single-point calculations were also conducted on the B3LYP/6-311G(d,p) optimized structures using a self-consistent reaction field (SCRF) model. The SCRF methods treat the solute at the quantum mechanical level, while the solvent is represented as a dielectric continuum. Specifically, we chose the polarizable continuum model (PCM) developed by Tomasi and co-workers to describe the bulk solvent.[17,18] The PCM method involves the generation of a solvent cavity from spheres centered at each atom in the molecule and the calculation of virtual point charges on the cavity surface representing the polarization of the solvent. The magnitude of these charges is proportional to the derivative of the solute electrostatic potential at each point calculated from the molecular wave function. The point charges may, then, be included in the one-electron Hamiltonian, thus inducing polarization of the solute. An iterative calculation is carried out until the wave function and the surface charges are self-consistent. PCM calculations were also performed in the framework of the DFT B3LYP/6-311G-(d,p) level using the standard protocol and considering the dielectric constants of chloroform ($\epsilon = 4.9$) and water ($\epsilon = 78.4$). The conformational free energies in chloroform and aqueous solutions (ΔG^{CHL} and ΔG^{WAT}, respectively) were computed using the classical thermodynamics scheme: the free energies of solvation ($\Delta G_{sol/CHL}$ and $\Delta G_{sol/WAT}$) provided by the PCM model were added to the ΔG^{gp}:

$$\Delta G^{CHL} = \Delta G_{sol/CHL} + \Delta G^{gp} \qquad (3)$$

$$\Delta G^{WAT} = \Delta G_{sol/WAT} + \Delta G^{gp} \qquad (4)$$

MD simulations in both chloroform and water solutions were performed using the NAMD program.[19] The simulated peptide $Ac-Ac_5c-NHMe$ was placed in the center of a cubic simulation box ($a = 31.1$ Å) filled with explicit solvent molecules (293 and 951 for chloroform and water, respectively). The water molecules were represented using the TIP3 model,[20] while chloroform was described using the OPLS4 model.[21] Atom pair distance cutoffs were applied at 14 Å to compute van der Waals interactions. The electrostatic interactions were computed using the nontruncated electrostatic potential by means of Ewald

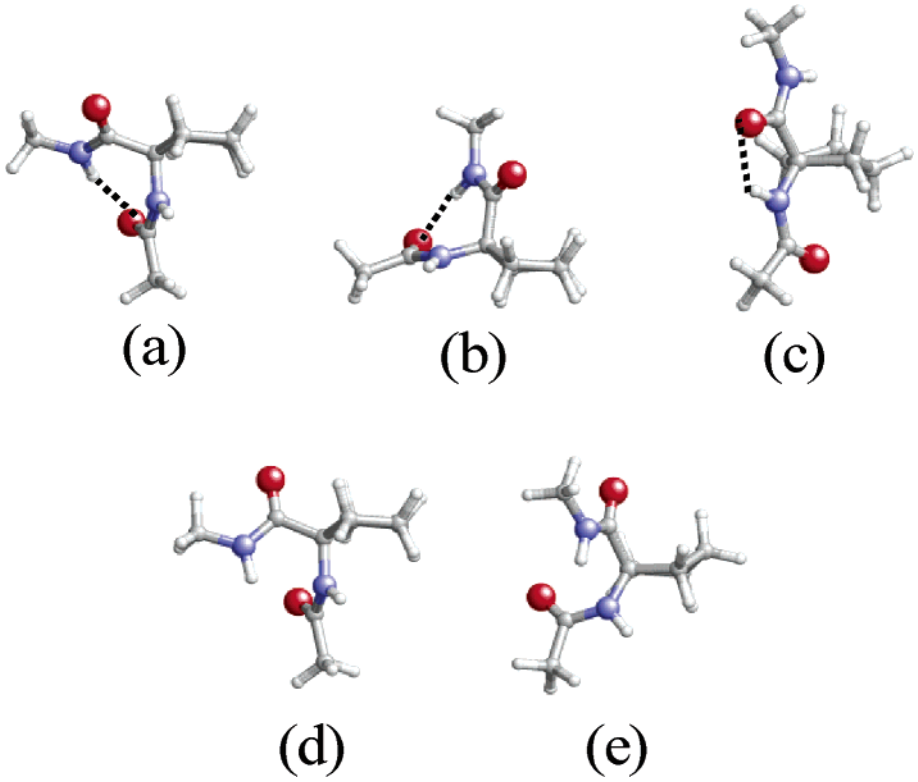

Figure 2. Minimum energy conformations of Ac−Ac$_5$c−NHMe at the B3LYP/6-311G(d,p) level: (a) $C_7/^{\alpha}E$; (b) $C_7/_{\alpha}E$; (c) $C_5/^{\gamma}_{\gamma'}T$; (d) $\alpha/^{\alpha}E$; (e) $\alpha/_{\gamma}E$. The parameters associated with N−H···O═C hydrogen bonds are given in the text.

TABLE 1: Backbone Torsion Angles, Endocyclic Torsion Angles, and Pseudorotational Phase Angle (*P*) for the Conformational Energy Minima of Ac−Ac$_5$c−NHMe at the B3LYP/6-311G(d,p) Level of Theory

	backbone torsion angles[a]				endocyclic torsion angles[a]					puckering[a]	
conformer	ω_0	φ	ψ	ω	χ^0	χ^1	χ^2	χ^3	χ^4	P	ΔE^b
$C_7/^{\alpha}E$	175.5	73.8	−56.5	−179.3	39.2	−26.1	2.8	21.8	−37.5	89.2	0.0
$C_7/_{\alpha}E$	177.3	75.4	−63.6	178.1	−41.5	31.4	−9.0	−16.9	36.0	267.3	0.4
$C_5/^{\gamma}_{\gamma'}T$	178.1	178.1	−175.7	179.7	−14.8	33.6	−39.4	30.3	−9.5	355.9	1.2
$\alpha/^{\alpha}E$	170.6	73.3	15.2	−177.6	39.4	−26.2	2.4	22.2	−37.9	89.3	2.7
$\alpha/_{\gamma}E$	169.6	68.1	24.4	−178.2	5.4	−29.0	41.8	−38.6	20.5	190.7	3.1

[a] In degrees. [b] Relative energy (in kcal/mol).

Summations. The real space term was determined by the van der Waals cutoff (14 Å), while the reciprocal term was estimated by interpolation of the effective charge into a charges mesh with a grid thickness of 5 points per volume unit, i.e., the Particle-Mesh Ewald (PME) method.[22] Bond lengths were constrained using the *SHAKE* algorithm[23] and the numerical integration step was 2 fs.

Before the MD run series was started, 5×10^3 steps of energy minimization were performed to relax conformational and structural tensions. Different consecutive rounds of short MD runs were performed to equilibrate the density, temperature, and pressure: 0.50 ns of *NVT*-MD at 298 K (thermal relaxation) followed by 0.25 ns of isobaric relaxation (*NPT*-MD). Both temperature and pressure were controlled by the weak coupling method, the Berendsen thermo-barostat[24] using a time constant for heat bath coupling, and a pressure relaxation time of 1 ps. The coordinates of the *NPT*-MD production runs, which were 15 ns long, were saved every 500 steps (1 ps intervals) for subsequent analysis.

Results and Discussion

Conformational Properties. Geometry optimizations in the gas phase at the B3LYP/6-311G(d,p) level of the 18 structures considered as starting geometries (see Methods) led to five different minimum energy structures for Ac−Ac$_5$c−NHMe. Table 1 lists the backbone torsion angles, the side-chain endocyclic torsion angles, and the pseudorotational phase angle of such minima, which are represented in Figure 2. Table 2 shows the conformational free energies in the gas phase.

TABLE 2: Relative Conformational Free Energies[a] at 298 K for the Minima of Ac−Ac$_5$c−NHMe in the Gas Phase, Chloroform Solution, and Aqueous Solution (ΔG^{gp}, ΔG^{CHL}, and ΔG^{WAT}, Respectively); Solvation Free Energies[a] in Chloroform and Aqeuous Solutions Are Also Displayed ($\Delta G_{sol/CHL}$ and $\Delta G_{sol/WAT}$, Respectively)

conformer	ΔG^{gp}	$\Delta G_{sol/CHL}$	ΔG^{CHL}	$\Delta G_{sol/WAT}$	ΔG^{WAT}
$C_7/^{\alpha}E$	0.0	−6.7	0.0	−10.3	0.2
$C_7/_{\alpha}E$	0.6	−6.4	0.9	−10.1	1.0
$C_5/^{\gamma}_{\gamma'}T$	1.8	−5.4	3.1	−8.8	3.5
$\alpha/^{\alpha}E$	2.4	−7.5	1.6	−12.9	0.0
$\alpha/_{\gamma}E$	3.1	−7.9	1.9	−13.4	0.1

[a] In kcal/mol.

The lowest energy conformation in the gas phase corresponds to the $C_7/^{\alpha}E$ (Figure 2a) in which the backbone dihedral angles φ,ψ define a seven-membered intramolecularly hydrogen-bonded ring (C_7) or γ-turn conformation with parameters d(H···O) = 1.903 Å and −N−H···O = 152.2° and the cyclopentane

ring adopts a C^{α}-*endo* envelope ($^{\alpha}$E) arrangement. The most relevant difference between the global minimum and the $C_7/_{\alpha}E$ minimum (Figure 2b) [d(H···O) = 1.928 Å and −N−H···O = 149.7°] concerns the cyclopentane ring, which in the latter adopts a C^{α}-*exo* envelope ($_{\alpha}$E) arrangement. This disposition of the cyclic side chain is responsible for the unfavorable interaction between the carbonyl oxygen of the Ac_5c residue and H−C^{β} that induces a destabilization in the free energy of 0.6 kcal/mol (Table 2).

In the next minimum, named as $C_5/^{\gamma}_{\gamma}T$ (Figure 2c), the amide moieties define a five-membered intramolecularly hydrogen-bonded ring (C_5) with d(H···O) = 2.010 Å and −N−H···O = 112.7°, while the cyclopentane is arranged in a C^{γ}-*endo*-$C^{\gamma'}$-*exo* twist ($^{\gamma}_{\gamma}$T) disposition. This structure is unfavored with respect to the global minimum by 1.8 kcal/mol. Such a feature should be mainly attributed to the stability of the C_5 conformation, which is lower than that of the C_7. Recent calculations at the B3LYP/6-31G(d) level on Ac−Ac_3c−NHMe indicated that the C_5 minimum is unfavored with respect to the C_7 by 2.5 kcal/mol.[5c] Accordingly, the energy difference between the C_7 and C_5 conformations seems to increase with the strain of the cycloalkane ring.

Finally, the backbone of the last two minima corresponds to a 3_{10}-/α-helical conformation (α), while the cyclic side chain adopts either a C^{α}-*endo* ($^{\alpha}$E) or a C^{γ}-*exo* ($_{\gamma}$E) arrangement. The $\alpha/^{\alpha}E$ conformation (Figure 2d) is unfavored with respect to the global minimum by 2.4 kcal/mol, while the $\alpha/_{\gamma}E$ (Figure 2e) is further destabilized by 0.7 kcal/mol due to the repulsive interaction between the carbonyl moiety of the Ac_5c residue and the side group.

It should be noted that all the conformations listed in Table 1 are 2-fold degenerate because of the achiral nature of the compound; i.e., equivalent conformations are generated by changing the sign of all the backbone and endocyclic dihedral angles: $\varphi,\psi,\{\chi^i\} = -\varphi,-\psi,\{-\chi^i\}$.

Table 2 compares the conformational free energies in the gas phase with those estimated in chloroform and aqueous solutions, the solvation free energies being also displayed. As expected, the free energies of solvation indicate that interaction of the solute is more favorable with water than with chloroform. However, the most remarkable feature of Table 2 is the crucial role played by the environment in the stability of the different minima. Thus, although the solute−solvent interactions follow the same relative order in the two solvents ($\alpha/_{\gamma}E$ > $\alpha/^{\alpha}E$ > $C_7/^{\alpha}E$ > $C_7/_{\alpha}E$ > $C_5/^{\gamma}_{\gamma}T$), the magnitude of such interactions strongly depends on the polarity of the solvent. For instance, the difference between the free energies of solvation of the best and worst solvated conformations is only 2.5 kcal/mol in chloroform solution, while it grows to 4.6 kcal/mol in water. Consequently, the conformational preferences in aqueous solution are very different not only from those obtained in the gas phase but also from those in chloroform. Thus, in the latter environment the lowest energy conformation is the same as that in the gas phase, even though the two helical conformations become more stable than the $C_5/^{\gamma}_{\gamma}T$. In contrast, the $\alpha/_{\gamma}E$, $\alpha/^{\alpha}E$, and $C_7/^{\alpha}E$ conformations are almost isoenergetic in aqueous solution, while the $C_7/_{\alpha}E$ and $C_5/^{\gamma}_{\gamma}T$ are destabilized by 1.0 and 3.5 kcal/mol, respectively.

Pseudorotation of the Cyclic Side Chain. Figure 3a shows a plot of the B3LYP/6-311G(d,p) relative energies in the gas phase as a function of the phase angle of pseudorotation for the C_7, C_5, and α backbone conformations of Ac−Ac_5c−NHMe. As can be seen, the dependence of the profiles upon the backbone conformation is dramatic. The lowest energy pseudorotation path corresponds exclusively to the C_7 conformation, the highest pseudorotational barrier being 0.8 kcal/mol for P = 0° ($^{\gamma}_{\gamma}$T). The second barrier, which appears at P = 234° (C^{β}-*endo*; $^{\beta}$E), is well-defined with 0.6 kcal/mol. Finally, the position and the relative stability of both the $^{\alpha}$E and $_{\alpha}$E minima are fully consistent with the results displayed in Table 1. As can be seen, the energy of all the cyclopentane arrangements described by the pseudorotational path is sufficiently low to be considered as accessible states at room temperature.

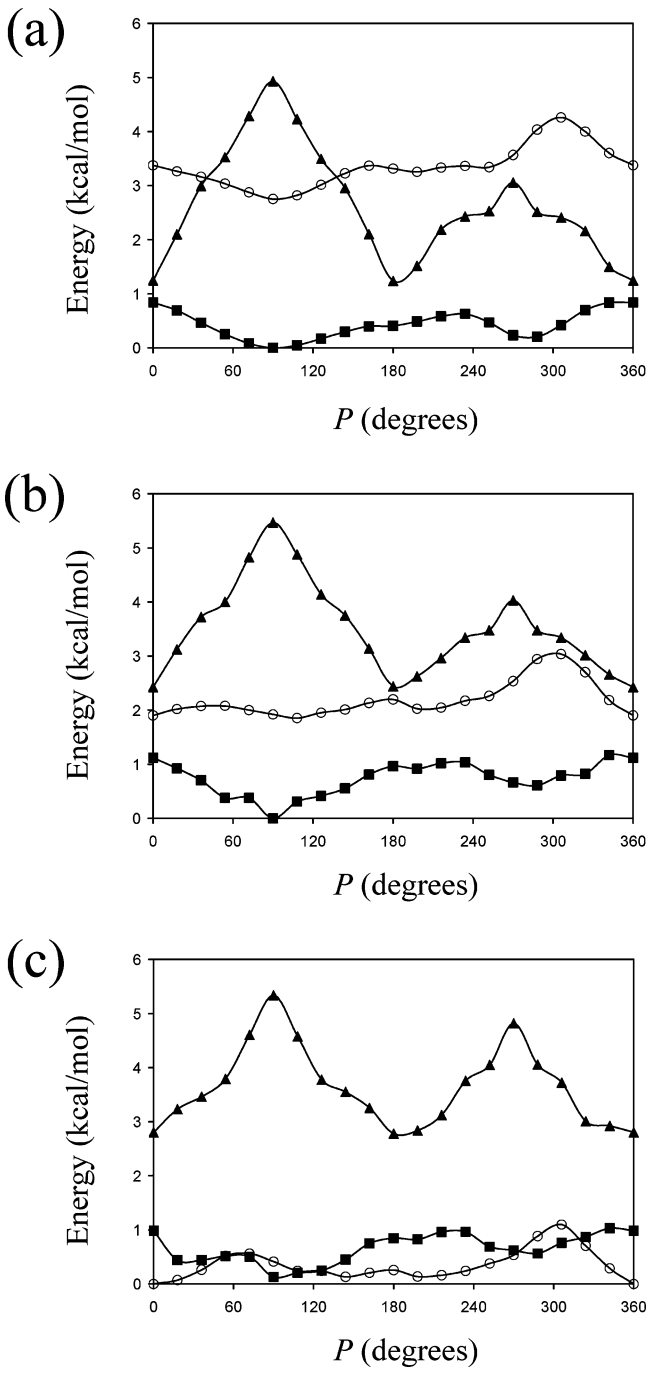

Figure 3. Plots of the relative B3LYP/6-311G(d,p) energy as a function of the phase angle of pseudorotation (P) for the C_7 (filled squares), C_5 (filled triangles), and α (empty circles) backbone conformations of Ac−Ac_5c−NHMe. The plots correspond to the potential energy curves calculated in the (a) gas phase, (b) chloroform solution, and (c) water solution.

For the C_5 conformation, the plot shows two minima located at P = 0° and 180°: the former corresponds to the structure described in Table 1, i.e., $C_5/^{\gamma}_{\gamma}T$, while the latter is its mirror

image ($C_5/^{\gamma'}_{\gamma}T$). Accordingly, both structures are isoenergetic and must be considered as equivalent. These two twisted arrangements are separated by the $^{\alpha}E$ ($P = 90°$) and $_{\alpha}E$ ($P = 270°$) barriers that are 3.7 and 1.8 kcal/mol higher in energy, respectively, indicating that the interconversion between the $^{\gamma}_{\gamma'}T$ and $^{\gamma'}_{\gamma}T$ arrangements occurs preferentially through the latter. It is worth noting that the asymmetry in the chemical structure of the peptide backbone is responsible for the difference between the energetic profiles associated with the regions that separate the two minima, i.e., the regions with P ranging from 18° to 162° and from 198° to 342°. For instance, the interaction between the cycle and the peptide backbone is expected to be clearly different for the $^{\alpha}E$ ($P = 90°$) and the $_{\alpha}E$ ($P = 270°$) arrangements; i.e., in the former conformation the cyclopentane moiety mainly interacts with the NHMe amide hydrogen while in the latter the interaction occurs with the carbonyl oxygen of the acetyl group. Furthermore, it should be noted that many of the conformers described in the C_5 profile are destabilized with respect to the global minimum of the C_7 conformation by more than 1.5 kcal/mol.

On the other hand, the puckering arrangements contained in the α profile are destabilized with respect to those of the C_7 curve by at least 2.7 kcal/mol, indicating that the former are inaccessible states at room temperature. However, it is worth noting that the profile obtained for the α conformer is flatter than that of the C_5. Thus, the barriers at $P = 144°$ and 306° are 0.5 and 1.5 kcal/mol, respectively, higher in energy than the lowest energy minimum found at $P = 90°$.

Figured 3b and 3c represent the pseudorotational potential energies in chloroform and aqueous solutions, respectively. As can be seen, the general trends of the curves are similar to those described above for the gas phase. However, there is a feature of particular relevance: the stability of the cyclopentane arrangements associated with the α conformation increases with the polarity of the solvent. Thus, the whole pseudorotational α profile becomes more stable than the C_5 profile in chloroform solution, while in water the α and C_7 curves are within the same range of energies. Furthermore, the potential energies in the latter profiles are under 1.1 kcal/mol, indicating that in aqueous solution all the pesudorotational states can exist at room temperature for both the C_7 and α backbone conformations.

Figure 4 shows the variation of the optimized backbone dihedral angles φ and ψ in the gas phase against the phase angle of pseudorotation for the three conformations considered. The largest variation corresponds to the C_5 conformation for both φ and ψ, the difference between the highest and lowest values of these dihedrals being $\Delta\varphi = 41.9°$ and $\Delta\psi = 43.4°$. However, it should be remarked that such variations are not large enough to abandon the C_5 conformation. On the other hand, the fluctuations of the backbone dihedral angles were significantly smaller for the C_7 ($\Delta\varphi = 2.9°$ and $\Delta\psi = 7.6°$) and α conformations ($\Delta\varphi = 6.8°$ and $\Delta\psi = 17.1°$). The behavior shown by the three backbone conformations is fully consistent with the potential energy curves displayed in Figure 3. Thus, the C_5 conformation exhibits the wider energy regions along the pseudorotational path, which explains the distortions in the backbone dihedral angles during their exploration. Overall, these results indicate that the pseudorotational equilibrium associated with the cyclopentane does not perturb the backbone conformation, especially for the C_7 and α minima.

Force-Field Parametrization. In Ac_3c, hyperconjugation occurs between the lone pairs of the carbonyl oxygen and the σ^* $C^{\beta}-C^{\beta'}$ molecular orbital of the cyclopropane ring. To consider appropriately this electronic effect in MD simulations,

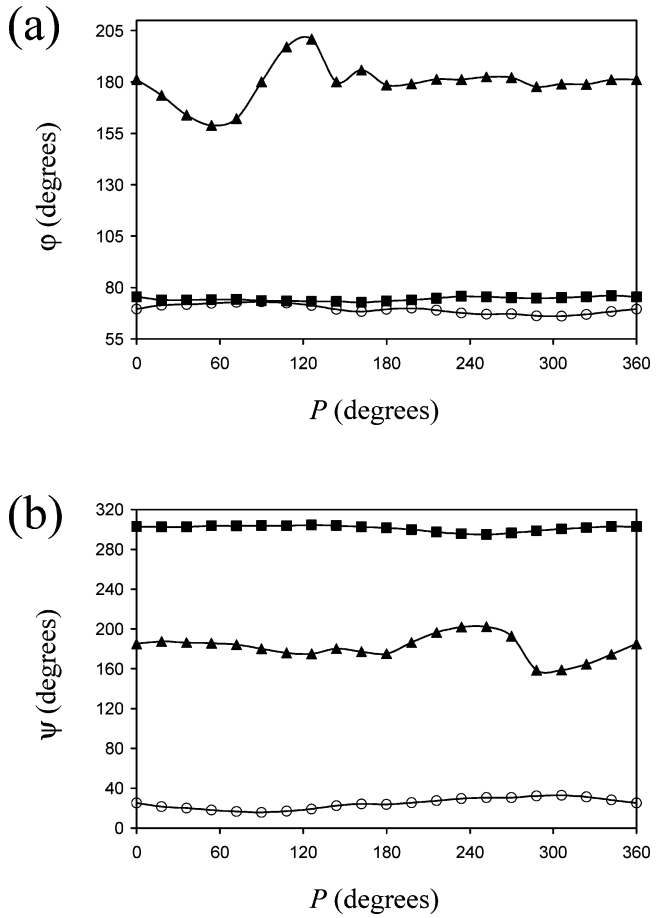

Figure 4. Dependence of the backbone dihedral angles φ (a) and ψ (b) with the phase angle of pseudorotation (P) for the C_7 (filled squares), C_5 (filled triangles), and α (empty circles) conformations of Ac−Ac_5c−NHMe. To avoid discontinuities, the values of φ and ψ are represented from 0° to 360° rather than from −180° to 180°.

a specific force-field parametrization was developed to represent the stretching, bending, torsional, and electrostatic interactions of this amino acid.[5b,24] In contrast, no special electronic effect has been detected for Ac−Ac_5c−NHMe. Therefore, electrostatic charges have been the only force-field parameters specifically developed for Ac_5c, the stretching, bending, torsional, and van der Waals parameters being directly transferred from the Amber force field.[26]

Atomic charges for the five minimum energy conformations listed in Table 1 were calculated by fitting the HF/6-31G(d) quantum mechanical and the Coulombic molecular electrostatic potentials (MEPs) to a large set of points placed outside the nuclear region. It should be noted that the electrostatic parameters derived at this level of theory are fully compatible with the current Amber force field.[26] Electrostatic potential (ESP) fitting atomic centered charges for the Ac_5c residue were derived by weighing the charges calculated for the five minimum energy conformations according to the Boltzmann populations. The weights were given by the standard Boltzmann formula using the ΔG^{gp} values listed in Table 2. The resulting electrostatic parameters are displayed in Figure 5.

An important test to check the reliability of force-field parameters developed for amino acids is the attempt to reproduce the minimum energy conformations of dipeptides.[26,27] Table 3 compares the quantum mechanical energies of the five minimum energy conformations predicted for Ac−Ac_5c−NHMe with the classical energies obtained in the gas phase using the force-field parameters discussed above. As can be seen, the agreement

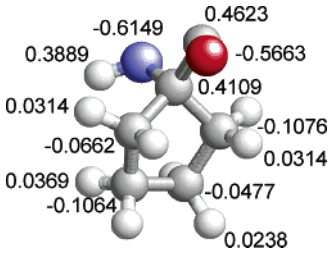

Figure 5. Electrostatic parameters determined for the Ac_5c residue.

TABLE 3: Conformational Energies of Ac−Ac_5c-NHMe (in kcal/mol)

	$C_7/^{\alpha}E$	$C_7/_{\alpha}E$	$C_5/^{\gamma}_{\gamma'}T$	$\alpha/^{\alpha}E$	$\alpha/_{\gamma}E$
E(MM)[a]	0.0	0.7	2.2	5.0	6.3
E(QM)[b]	0.0	0.4	1.2	2.7	3.1

[a] Force-field energies calculated using the parameters discussed in the text. [b] Quantum mechanical energies calculated at the B3LYP/6-311G(d,p) level.

with the B3LYP/6-311G(d,p) data is very good. Thus, the relative energy order provided by classical mechanics and DFT calculations is the same. Indeed, the most important difference between the two sets of energies refers to the stability of the α conformations, which is underestimated by force-field calculations. However, it is noticeable that Kollman and co-workers detected the same deficiency for the glycine dipeptide.[26]

To ascertain how the force-field parameters describe the conformational flexibility of Ac−Ac_5c−NHMe in solution, MD simulations were performed at 298 K in both chloroform and aqueous solutions. In both cases the lowest energy conformation was used as a starting point, each trajectory being 15 ns long. Figure 6 represents the accumulated Ramachandran plot for the Ac_5c dipeptide. It is worth noting that in chloroform only the C_7 and α regions are populated, while in water the C_5 conformation is detected occasionally. These results, which are in excellent agreement with the ΔG^{CHL} and ΔG^{WAT} values derived from DFT calculations (Table 2), indicate that the Ac_5c force-field parameters are able to describe correctly the conformational preferences of this amino acid.

Regarding the pseudorotation of the cyclic side chain, the most populated values of the pseudorotation phase angle were determined as a function of the backbone conformation by analyzing the snapshots recorded from the MD simulations. Results are compared in Table 4 with those derived from DFT calculations. As can be seen, the description provided by the classical force field of the different pseudorotational states is only satisfactory for the minimum energy arrangements, whose populations are clearly overestimated. Accordingly, many of the low-energy regions predicted at the DFT level, which are close to the energy minima (Figure 3), were not visited during the MD simulations. This was an expected result since the main objective of the potential energy terms used in first-class force fields is to describe satisfactorily the minimum energy arrangements. Thus, the equilibrium geometric parameters, i.e., bond lengths and bond angles, are usually extracted from structures determined by X-ray crystallography, which are free energy minima, or alternatively from minimum energy conformations derived from quantum mechanical calculations. Furthermore, equilibrium parameters remain fixed during the whole MD simulations, no variation with the conformation being allowed. Additionally, it should be noted that electrostatic parameters, which are essential in MD simulations of peptides and proteins, are usually derived using the geometries of the quantum mechanical minimum energy conformations of the amino acids.

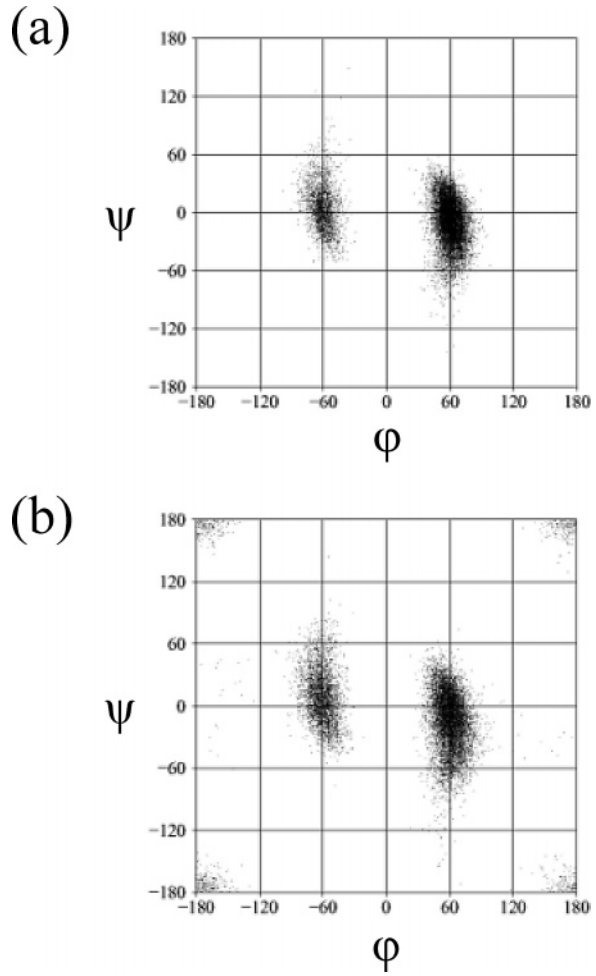

Figure 6. Accumulated Ramachandran plot for Ac−Ac_5c−NHMe derived from MD trajectories 15 ns long in chloroform (a) and aqueous (b) solutions.

Considering the large number of approximations included in force-field simulations and taking into account the complexity of the pseudorotational equilibrium of the cyclopentane ring in Ac_5c, we feel that the right description of the minimum energy states displayed in Table 4 is a good result.

Conclusions

DFT calculations on Ac−Ac_5c−NHMe at the B3LYP/6-311G(d,p) level allow us to draw the following conclusions about the conformational preferences of this constrained amino acid:

(i) Its cyclic side chain restricts the conformational flexibility of the backbone. Thus, only the C_7, C_5, and α conformations were identified as energy minima, the ΔG^{gp} of the latter two being higher than 1.8 kcal/mol.

(ii) The pseudorotational cyclopentane puckering strongly depends on the peptide backbone structure. Thus, the potential energy surfaces obtained for the C_7, C_5, and α conformations indicate that the arrangement of the cyclopentane ring is determined by interactions between the side chain and the backbone.

(iii) Both the backbone conformation and the pseudorotational puckering of the cyclic side chain are strongly influenced by the polarity of the solvent. Thus, in aqueous solution the C_7 and α minima are isoenergetic, while in chloroform the C_7 is clearly preferred. On the other hand, all the pseudorotational states compatible with the C_7 and α conformations can exist in

TABLE 4: Populations of the More Visited Pseudorotational Ring Puckerings during the MD Simulations; Quantum Mechanical (QM) Populations Are Included for Comparison

back bone	environ-ment	P (deg)[a]	population (%) QM[b]/MD[c]	P (deg)	population (%) QM[b]/MD[c]
C_7	chloroform	90	14.4/49.8	290	5.1/32.5
	water	90	10.4/43.4	290	5.0/20.6
C_5	chloroform	0	14.4/—[d]		
	water	0	11.3/—[d]		
a	chloroform	108	7.5/39.7	198	5.6/33.3
	water	18	6.9/31.2	198	6.2/29.1

[a] The snapshots recorded from MD simulations were categorized as a function of the pseurotational phase angle and the backbone conformation, a tolerance of ±9° being allowed for the P values. Quantum mechanical results were derived from the profiles shown in Figure 3 assuming a Boltzmann distribution. [b] From B3LYP/6-311G(d,p) quantum mechanical calculations. [c] From MD simulations. [d] The number of visits to the C_5 conformation during the MD simulations is not representative.

water at room temperature, while only those of the C_7 structure are accessible in chloroform.

(iv) Classical simulations in aqueous and chloroform solutions using a set of force-field parameters, which was obtained by combining explicitly developed electrostatic potential to fit atomic centered charges with parameters directly transferred from the Amber force field, are able to describe satisfactorily the minimum energy conformations of the Ac_5c in terms of both backbone and cyclopentane ring puckering.

Acknowledgment. Authors are indebted to the Centre de Supercomputació de Catalunya (CESCA) for computational resources. We acknowledge the National Cancer Institute for partial allocation of computing time and staff support at the Advanced Biomedical Computing Center of the Frederick Cancer Research and Development Center. Classic calculations were partially formed by utilizing the high-performance computational capabilities of the Biowulf PC/Linux cluster at the National Institutes of Health, Bethesda, MD (http://biowulf.nih.gov). D.Z. is thankful for financial support from the Ramon y Cajal program of the Spanish "*Ministerio de Educación y Ciencia*" (MEC). This project has been funded in whole or in part with Federal funds from the National Cancer Institute, National Institutes of Health, under Contract Number N01-CO-12400. The content of this publication does not necessarily reflect the view of the policies of the Department of Health and Human Services, nor does mention of trade names, commercial products, or organization imply endorsement by the U.S. Government. This research was supported [in part] by the Intramural Research Program of the NIH, National Cancer Institute, Center for Cancer Research.

References and Notes

(1) (a) Carlson, K. L.; Lowe, S. L.; Hoffmann, M. R.; Thomasson, K. A. *J. Phys. Chem. A* **2006**, *110*, 1925. (b) Kang, Y. K. *J. Mol. Struct. (THEOCHEM)* **2004**, *675*, 1. (c) Kang, Y. K. *J. Phys. Chem. B* **2004**, *108*, 5463. (d) Czinki, E.; Császár, A. G. *Chem. Eur. J.* **2003**, *9*, 1008. (e) Improta, R.; Benzi, C.; Barone, V. *J. Am. Chem. Soc.* **2001**, *123*, 12568. (f) Stephanian, S. G.; Reva, I. D.; Radchenko, E. D.; Adamowicz, L. *J. Phys. Chem. A* **2001**, *105*, 10664. (g) Császár, A. G.; Perczel, A. *Prog. Biophys. Mol. Biol.* **1999**, *71*, 243. (h) Badoni, H. A.; Rodriguez, A. M.; Zamora, M. A.; Zamarbide, G. N.; Enriz, R. D.; Farkas, Ö; Császar, P.; Torday, L. L.; Sosa, C. P.; Jakli, I.; Perczel, A.; Papp, J. G.; Hollosi, M.; Csizmadia, I. G. *J. Mol. Struct. (THEOCHEM)* **1999**, *465*, 79. (i) Ramek, M.; Kelterer, A.-M.; Teppen, B.; Schäfer, L. *J. Mol. Struct.* **1995**, *352/353*, 59.

(2) (a) Lesarri, A.; Cocinero, E. J.; López, J. C.; Alonso, J. L. *J. Am. Chem. Soc.* **2005**, *127*, 2572. (b) Song, K. I.; Kang, Y. K. *J. Phys. Chem. B* **2005**, *109*, 16982. (c) Lam, J. S. W.; Koo, J. C. P.; Hudáky, I.; Varro, A.; Papp, J. G.; Penke, B.; Csizmadia, I. G. *J. Mol. Struct. (THEOCHEM)* **2003**, *666*, 285. (d) Benzi, C.; Improta, R.; Scalmani, G.; Barone, V. *J. Comput. Chem.* **2002**, *23*, 341.

(3) Alemán, C.; Zanuy, D.; Jiménez, A. I.; Cativiela, C.; Haspel, N.; Zheng, J.; Casanovas, J.; Wolfson, H.; Nussinov, R. *Phys. Biol.* **2006**, *3*, S54−S62.

(4) (a) Toniolo, C.; Crisma, M.; Formaggio, F.; Peggion, C. *Biopolymers (Pept. Sci.)* **2001**, *60*, 396. (b) Benedetti, E. *Biopolymers (Pept. Sci.)* **1996**, *40*, 3. (c) Valle, G.; Crisma, M.; Toniolo, C.; Holt, E. M.; Tamura, M.; Bland, J.; Stammer, C. H. *Int. J. Pept. Protein Res.* **1989**, *34*, 56. (d) Benedetti, E.; Di Blasio, B.; Pavone, V.; Pedone, C.; Santini, A.; Barone, V.; Fraternalli, E. F.; Lelj, F.; Bavoso, A.; Crisma, M.; Toniolo, C. *Int. J. Biol. Macromol.* **1989**, *11*, 353.

(5) (a) Alemán, C. *J. Phys. Chem. B* **1997**, *101*, 5046. (b) Gómez-Catalán, J.; Alemán, C.; Pérez, J. J. *Theor. Chem. Acc.* **2000**, *103*, 380. (c) Alemán, C.; Jiménez, A. I.; Cativiela, C.; Pérez, J. J.; Casanovas, J. *J. Phys. Chem. B* **2002**, *106*, 11849.

(6) (a) Aschi, M.; Lucente, G.; Mazza, F.; Mollica, A.; Morera, E.; Nalli, M.; Paglialunga Paradisi, M. *Org. Biomol. Chem.* **2003**, *1*, 1980. (b) Santini, A.; Di Blasio, B.; Galdiero, S.; Iacovino, R.; Pedone, C.; Benedetti, E.; Crisma, M.; Toniolo, C. *Z. Kristallogr.* **1996**, *211*, 616. (c) Santini, A.; Barone, V.; Bavoso, A.; Benedetti, E.; Di Blasio, B.; Fraternalli, F.; Lelj, F.; Pavone, V.; Pedone, C.; Crisma, M.; Bonora, G. M.; Toniolo, C. *Int. J. Biol. Macromol.* **1988**, *10*, 292. (d) Crisma, M.; Bonora, G. M.; Toniolo, C.; Benedetti, E.; Bavoso, A.; Di Blasio, B.; Pavone, V.; Pedone, C. *Int. J. Biol. Macromol.* **1988**, *10*, 300. (e) Valle, G.; Crisma, M.; Toniolo, C. *Can. J. Chem.* **1988**, *66*, 2575. (f) Bardi, R.; Piazzesi, A. M.; Toniolo, C.; Sukumar, M.; Balaram, P. *Biopolymers* **1986**, *25*, 1635.

(7) Kilpatrick, J. E.; Pitzer, K. S.; Spitzer, R. *J. Am. Chem. Soc.* **1947**, *69*, 2483.

(8) Frisch, M. J.; Trucks, G. W.; Schlegel, H. B.; Scuseria, G. E.; Robb, M. A.; Cheeseman, J. R.; Montgomery, J. A.; Vreven, T., Jr.; Kudin, K. N.; Burant, J. C.; Millam, J. M.; Iyengar, S. S.; Tomasi, J.; Barone, V.; Mennucci, B.; Cossi, M.; Scalmani, G.; Rega, N.; Petersson, G. A.; Nakatsuji, H.; Hada, M.; Ehara, M.; Toyota, K.; Fukuda, R.; Hasegawa, J.; Ishida, M.; Nakajima, T.; Honda, Y.; Kitao, O.; Nakai, H.; Klene, M.; Li, X.; Knox, J. E.; Hratchian, H. P.; Cross, J. B.; Adamo, C.; Jaramillo, J.; Gomperts, R.; Stratmann, R. E.; Yazyev, O.; Austin, A. J.; Cammi, R.; Pomelli, C.; Ochterski, J. W.; Ayala, P. Y.; Morokuma, K.; Voth, G. A.; Salvador, P.; Dannenberg, J. J.; Zakrzewski, V. G.; Dapprich, S.; Daniels, A. D.; C. Strain, M.; Farkas, O.; Malick, D. K.; Rabuck, A. D.; Raghavachari, K.; Foresman, J. B.; Ortiz, J. V.; Cui, Q.; Baboul, A. G.; Clifford, S.; Cioslowski, J.; Stefanov, B. B.; Liu, G.; Liashenko, A.; Piskorz, P.; Komaromi, I.; Martin, R. L.; Fox, D. J.; Keith, T.; Al-Laham, M. A.; Peng, C. Y.; Nanayakkara, A.; Challacombe, M.; Gill, P. M. W.; Johnson, B.; Chen, W.; Wong, M. W.; Gonzalez, C.; Pople, J. A. *Gaussian 03*, revision B.02; Gaussian, Inc.: Pittsburgh, PA, 2003.

(9) Becke, A. D. *J. Chem. Phys.* **1993**, *98*, 1372.

(10) Lee, C.; Yang, W.; Parr, R. G. *Phys. Rev. B* **1993**, *37*, 785.

(11) McLean, A. D.; Chandler, G. S. *J. Chem. Phys.* **1980**, *72*, 5639.

(12) (a) Casanovas, J.; Jiménez, A. I.; Cativiela, C.; Pérez, J. J.; Alemán, C. *J. Org. Chem.* **2003**, *68*, 7088. (b) Casanovas, J.; Jiménez, A. I.; Cativiela, C.; Pérez, J. J.; Alemán, C. *J. Phys. Chem. B* **2006**, *110*, 5762.

(13) (a) Alemán, C.; Casanovas, J.; Zanuy, D.; Hall, H. K., Jr. *J. Org. Chem.* **2005**, *70*, 2950. (b) Alemán, C.; Casanovas, J.; Hall, H. K., Jr. *J. Org. Chem.* **2005**, *70*, 7731.

(14) Altona, C.; Sundaralingam, M. *J. Am. Chem. Soc.* **1972**, *92*, 8205.

(15) (a) Olson, W. K.; Sussman, J. L. *J. Am. Chem. Soc.* **1982**, *104*, 270. (b) Harvey, S.; Prabhakaran, M. *J. Am. Chem. Soc.* **1986**, *108*, 6128. (c) Shen, Q.; Mathers, T. L.; Raeker, T.; Hilderbrandt, R. L. *J. Am. Chem. Soc.* **1986**, *108*, 6888. (d) Plavec, J.; Tong, W.; Chattopadhyaya, J. *J. Am. Chem. Soc.* **1993**, *115*, 9734. (e) Gabb, H. A.; Lavery, R.; Prévost, C. *J. Comput. Chem.* **1995**, *16*, 667. (f) Brameld, K. A.; Goddard, W. A., III. *J. Am. Chem. Soc.* **1999**, *121*, 985.

(16) (a) Cremer, D.; Pople, J. A. *J. Am. Chem. Soc.* **1975**, *97*, 1354. (b) Kilpatrick, J. E.; Pitzer, K. S.; Spitzer, R. *J. Am. Chem. Soc.* **1947**, *69*, 2483.

(17) (a) Miertus, M.; Scrocco, E.; Tomasi, J. *Chem. Phys.* **1981**, *55*, 117. (b) Miertus, S.; Tomasi, J. *Chem. Phys.* **1982**, *65*, 239.

(18) (a) Tomasi, J.; Persico, M. *Chem. Rev.* **1994**, *94*, 2027. (b) Tomasi, J.; Mennucci, B.; Cammi, R. *Chem. Rev.* **2005**, *105*, 2999.

(19) Kale, L.; Skeel, R.; Bhandarkar, M.; Brunner, R.; Gursoy, A.; Krawetz, N.; Phillips, J.; Shinozaki, A.; Varadarajan, K.; Schulten, K. *J. Comput. Phys.* **1999**, *151*, 283.

(20) Jorgensen, W. L.; Chandrasekhar, J.; Madura, J. D.; Impey, R. W.; Klein, M. L. *J. Chem. Phys.* **1982**, *79*, 926.

(21) Jorgensen, W. L.; Briggs, J. M.; Contreras, M. L. *J. Phys. Chem.* **1990**, *94*, 1683.

(22) Darden, T.; York, D.; Pedersen, L. *J. Chem. Phys.* **1993**, *98*, 10089.

(23) Ryckaert, J. P.; Ciccotti, G.; Berendsen, H. J. C. *Comput. Phys.* **1990**, *94*, 1683.

(24) Berendsen, H. J. C.; Postma, J. P. M.; van Gunsteren, W. F.; DiNola, A.; Haak, J. R. *J. Chem. Phys.* **1984**, *81*, 3684.

(25) Alemán, C.; Galembeck, S. E.; Casanovas, J. *J. Comput.-Aided Mol. Design* **1998**, *12*, 259.

(26) Cornell, W. D.; Cieplak, P.; Bayly, C. I.; Gould, I. R.; Merz, K. M.; Ferguson, D. M.; Spellmeyer, D. C.; Fox, T.; Caldwell, J. W.; Kollman, P. A. *J. Am. Chem. Soc.* **1995**, *117*, 5179.

(27) (a) Weiner, S. J.; Kollman, P. A.; Nguyen, D. T.; Case, D. A. *J. Comput. Chem.* **1986**, *7*, 230. (b) Mackerrel, A. D., Jr.; Bashford, D.; Bellott, M.; Dunbrack, R. L., Jr.; Evanseck, J. D.; Field, M. J.; Fischer, S.; Gao, J.; Guo, H.; Ha, S.; Joseph-McCarthy, D.; Kuchnir, L.; Kuczera, K.; Lau, F. T. K.; Mattos, C.; Michnick, S.; Ngo, T.; Nguyen, D. T.; Prodhom, B.; Reiher, W. E., III; Roux, B.; Schlenkrich, M.; Smith, J. C.; Stote, R.; Straub, J.; Watanabe, M.; Wiórkieicz-Kuczera, J.; Yin, D.; Karplus, M. *J. Phys. Chem. B* **1998**, *102*, 3586. (c) Lii, J.-H.; Allinger, N. L. *J. Comput. Chem.* **1991**, *12*, 186.